JOURNAL OF GEOPHYSICAL RESEARCH, VOL. 105, NO. D21, PAGES 26,593–26,602, NOVEMBER 16, 2000

The effects of gravity waves on distributions of chemically active constituents in the mesopause region

Jiyao Xu

Laboratory of Numeric Study of Heliospheric Physics, Center for Space Science and Applied Research, Chinese Academy of Sciences, Beijing

Anne K. Smith and Guy P. Brasseur[1]

Atmospheric Chemistry Division, National Center for Atmospheric Research, Boulder, Colorado

Abstract. The influence of a monochromatic atmospheric gravity wave of fixed amplitude on the mean vertical distribution of mesospheric minor species is studied using a dynamical-photochemical gravity wave model. The fluctuations of winds, temperature, and species concentrations produced by the wave are calculated by a coupled linear gravity wave model. The effects of the wave on the mean mixing ratio of 19 key chemically active species is derived from a coupled system of continuity equations which accounts for full nonlinear photochemistry in a vertical column. This study focuses on the impact that gravity wave induced nonlinearities in the chemical reaction rates has on the chemical species distribution. The effects of gravity wave induced chemical transport and background diffusion are also calculated. Calculations indicate that the impacts of gravity waves on the vertical distribution (mean concentration) of atmospheric minor constituents are largest in the mesopause region, especially during nighttime. A comparison of the three effects indicates that for short lifetime chemical species such as O_3 and OH, the tendency due to chemical reaction perturbations induced by gravity waves is much greater than that due to transport and diffusion. The altitude range over which these nonlinearities is important is narrowly confined to the chemically active region near the mesopause.

1. Introduction

Atmospheric gravity waves are recognized as important, particularly in the upper mesosphere, where they provide much of the momentum forcing that drives the mean circulation. The characteristics of gravity waves, their contribution to the transport and dissipation of momentum and energy, the mechanisms and impact of their dissipation and breaking, and the influence of gravity waves on the atmospheric circulation have been the subject of many investigations [e.g., *Andrews and McIntyre*, 1976; *Lindzen*, 1981; *Dunkerton*, 1982; *Fritts*, 1984; *Smith et al.*, 1987; *Weinstock*, 1990].

The effect of atmospheric gravity waves on the distribution of minor atmospheric constituents has also been studied. Much of the theoretical and modeling work has been motivated by observations of airglow fluctuations as waves propagate vertically and has been focused on using airglow fluctuations to infer properties of the gravity waves themselves or the chemical processes involved in airglow [e.g., *Walterscheid et al.*, 1987; *Makhlouf et al.*, 1995; *Makhlouf et al.*, 1998; *Swenson and Gardner*, 1998]. There have also been models of the details of transport of conserved and chemically active trace species for realistic gravity waves [e.g., *Eckermann et al.*, 1998; *Fritts et al.*, 1997].

In studies that focus on the chemical composition, a dominant impact of gravity waves is the vertical mixing generated by wave breaking and by organized (advective) vertical mass transport. These are often represented as vertical diffusion of trace species [*Allen et al.*, 1981; *Garcia and Solomon*, 1985] since the exchange of air will tend to mix chemical species that have significant gradients. However, *Strobel* [1981] noted that the strong coupling between chemistry and temperature through the temperature dependence of chemical reaction rates affects the net vertical wave transport of minor constituents. *Schoeberl et al.* [1983] and *Strobel et al.* [1987] simulated this effect for transport of heat and chemical species and compared it with the diffusion by breaking gravity waves. They found that the chemical transport effect acts to augment the net mass transport

[1]Also at Max Planck Institute for Meteorology, Hamburg, Germany

Paper number 2000JD900446.
0148-0227/00/2000JD900446$09.00

for a few species and can result in a factor of two amplification in the tendency to the background concentration. In these studies, the chemical source/sink terms were assumed to be represented by linear loss rates.

Walterscheid and Schubert [1989] have also studied the gravity wave induced transport of active chemical species using a model which represents five species in the oxygen and hydrogen family at the nightside mesopause. The chemical interactions simulated in their model were simplified and perturbations to the photochemical rates were parameterized. They found that gravity waves can influence the mean profiles of O_3 and OH near the mesopause through nonlinear transport processes. The nonlinear effects can become dominant because there is a correlation between the vertical motion of the wave and the wave-induced perturbations in trace constituents. *Walterscheid and Schubert* [1989] pointed out that the effective net transport is not necessary down-gradient and therefore cannot be represented by vertical eddy diffusion.

Photochemical reactions are nonlinear processes and their rates depend sensitively on the densities of chemical species and on temperature. Therefore there can be significant variations in the production and loss rates of chemical species associated with gravity wave induced fluctuations in temperature and in the mixing ratios of interacting trace constituents. Representation of the mean photochemical production or loss rate by the product of mean species concentrations may introduce substantial errors.

In this paper we extend the previous studies [*Strobel*, 1981; *Walterscheid and Schubert*, 1989] but focus mainly on the impact of nonlinear photochemical reactions associated with gravity waves on the chemical species distribution. This process occurs when changes in temperature or in the concentrations of a trace species have significant impact on the production or loss of another species. We use a full nonlinear photochemistry model to assess the importance of this effect in the mesopause region. Comparison of the impact of this effect, the gravity wave induced chemical transport studied by *Strobel* [1981] and *Walterscheid and Schubert* [1989], and the diffusion induced by breaking gravity waves will be made.

2. Theory

Distributions of minor atmospheric constituents are determined by photochemical reactions, transport associated with resolved dynamical processes, and unresolved mixing process. The continuity equation for the species j in terms of mixing ratio can be written

$$\frac{\partial q_j}{\partial t} + \vec{V} \cdot \nabla q_j = \frac{1}{\rho_0}(P_j - L_j) + \frac{1}{\rho_0}\frac{\partial}{\partial z}\rho_0 K_z \frac{\partial q_j}{\partial z} \qquad j = 1, 2, 3, \ldots, J \tag{1}$$

where t is time; $\vec{V} = (u, v, w)$ is the vector wind velocity; u, v, and w are the wind velocities in x, y, and z directions, respectively; $q_j (j = 1, 2, ..., J)$ are the mixing ratios of the J chemical species; and ρ_0 is the background atmospheric density. $\vec{V} \cdot \nabla q_j$ represents the rate of change of the mixing ratio for species j due to resolved (advective) transport. P_j and L_j are the rates of change of species j due to photochemical production and loss. K_z is the vertical eddy diffusion coefficient, which accounts for vertical mixing due to unresolved processes (turbulence, gravity wave breaking, etc.).

Without loss of generality, the model fields can be split into mean and perturbation fields. Mean fields are denoted u_0, v_0, w_0, T_0, and $q_{0,j}$, and perturbation fields are u', v', w', T', q_j', etc. The production and loss rates are functions of rate coefficients or photolytic cross sections and one, two, or three concentrations for photolysis, two-body and three-body reactions, respectively. Perturbations in the photochemical production and loss terms can result from variations in temperature, which affect many of the reaction rates, and variations in the concentrations of one or more of the reactants. When written in terms of mean and perturbations, the continuity equation for species j becomes

$$\frac{\partial q_{0,j}}{\partial t} + \frac{\partial q_j'}{\partial t} + \vec{V_0} \cdot \nabla q_{0,j} + \vec{V'} \cdot \nabla q_{0,j} + \vec{V_0} \cdot \nabla q_j' + \vec{V'} \cdot \nabla q_j' =$$

$$\frac{1}{\rho_0}(P_{0,j} - L_{0,j}) + \frac{\partial}{\partial T}\left[\frac{1}{\rho_0}(P_{0,j} - L_{0,j})\right] T'$$

$$+ \sum_{k=1}^{J} \frac{\partial}{\partial q_{0,k}}\left[\frac{1}{\rho_0}(P_{0,j} - L_{0,j})\right] q_k'$$

$$+ \frac{1}{2}\left(T'\frac{\partial}{\partial T} + \sum_{k=1}^{J} q_k' \frac{\partial}{\partial q_{0,k}}\right)^2 \left[\frac{1}{\rho_0}(P_{0,j} - L_{0,j})\right]$$

$$+ \frac{1}{\rho_0}\frac{\partial}{\partial z}\rho_0 K_z \frac{\partial q_{0,j}}{\partial z}. \tag{2}$$

To determine the mean mixing ratio of species j, the time average of (2) is taken. For a coherent gravity wave, the time average of the first-order fluctuation terms over one wave period is zero, giving

$$\frac{\partial q_{0,j}}{\partial t} + \vec{V_0} \cdot \nabla q_{0,j} = \frac{1}{\rho_0}(P_{0,j} - L_{0,j}) + \mathcal{D}_j - \mathcal{T}_j + \mathcal{R}_j \tag{3}$$

where

$$\mathcal{D}_j = \frac{1}{\rho_0}\frac{\partial}{\partial z}\rho_0 K_z \frac{\partial q_{0,j}}{\partial z},$$

$$\mathcal{T}_j = \overline{\vec{V'} \cdot \nabla q_j'},$$

$$\mathcal{R}_j = \overline{\frac{1}{2}\left(T'\frac{\partial}{\partial T} + \sum_{k=1}^{J} q_k' \frac{\partial}{\partial q_{0,k}}\right)^2 \left[\frac{1}{\rho_0}(P_{0,j} - L_{0,j})\right]}.$$

This equation is formally similar to (1), with the addition of two terms that represent the impact of gravity waves on the time average distribution of chemical com-

pounds. Reading from left to right, the first four terms are similar to those in (1) and represent time tendency of the mean distribution, net advection by the background wind, photochemical sources and sinks based on the background composition and temperature, and the vertical diffusion term $\mathcal{D}_j$. The next two terms express the effect of gravity waves on the mean mixing ratio. The third term on the right side of (3), $\mathcal{T}_j$, represents the changes to the average atmospheric trace gas concentrations from the net advection produced by gravity wave winds. It is the gravity wave induced chemical transport or advection term. Some characteristics of this term have been studied by *Strobel* [1981] and *Walterscheid and Schubert* [1989]. They showed that it can make a significant contribution to the impact of gravity waves on the composition and can in some cases be larger than the effect of net mass transport by diffusion. The last term on the right side of (3), $\mathcal{R}_j$, is new and represents the changes in the average trace gas composition that occur when fluctuations in temperature and concentrations affect the net photochemical sources, and will be referred to as the gravity wave induced photochemical reaction term. As shown below, the magnitude of the gravity wave induced transport and photochemical reaction terms can become significant in the vicinity of the mesopause. Although the K_z term should also respond to gravity waves since K_z is enhanced when gravity waves break, in this study we specify a fixed K_z in order to concentrate on the effects of the gravity wave induced transport and photochemical reaction terms.

3. Numerical Model

This section describes a linear, three-dimensional coupled gravity wave and photochemical model that derives the gravity wave contributions to the tendency of mean concentrations. The model is three-dimensional in that it considers all three components of the gravity wave winds, but the background fields of temperature and trace species are assumed to have no horizontal gradients. The model proceeds in two steps. First, the background fields are defined. The dynamical background fields (T_0, $\vec{V}_0$, K_z) are specified, while the background chemical fields are determined with a one-dimensional photochemical model described below. Then the perturbation dynamical and chemical fields are determined from a coupled gravity wave calculation. These are used to calculate the magnitude and structure of the perturbation terms discussed in the previous section.

3.1. Chemical Scheme

The chemical scheme includes 19 species belonging to the oxygen (O_3, $O(^3P)$, $O(^1D)$), hydrogen (H, OH, HO_2, HO_2NO_2, H_2O_2), nitrogen (N, NO, NO_2, NO_3, N_2O_5, HNO_3), and chlorine (Cl, ClO, HCl, HOCl,

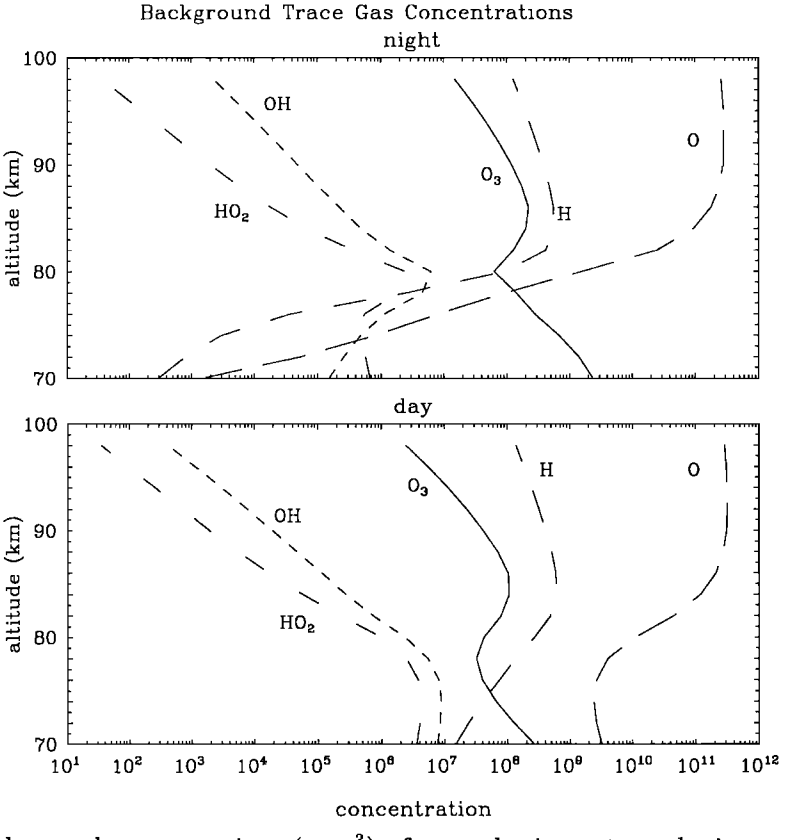

Figure 1. Background concentrations (cm^{-3}) of several minor atmospheric constituents as a function of altitude (kilometers) in the mesopause region at (top) midnight and (bottom) midday.

$ClONO_2$) families. Concentrations of several longer-lived species (O_2, N_2, H_2, CO_2, CO, CH_4, N_2O and H_2O) are specified using distributions from *Brasseur and Solomon* [1986]. The chemical rate constants are taken from *DeMore et al.* [1997] where available and in a few cases are taken from *Brasseur and Solomon* [1986].

Figure 1 shows model calculated background profiles of $O(^3P)$, O_3, H, OH, and HO_2 at midday and midnight between 70 and 100 km. These five compounds are considered here because they control photochemical processes in this altitude range and their concentrations can be highly variable. The calculation has been performed for equinox conditions at 45°N. The calculated density of $O(^3P)$ is about 3.2×10^{11} cm^{-3} at midday and 2.9×10^{11} cm^{-3} at midnight in the region of the mesopause, which compares well with the mean value of 3.5×10^{11} cm^{-3} at 40°N and 50°N in March from the reference model of *Llewellyn and McDade* [1996]. The ozone density calculated at 86 km is about 1.1×10^8 cm^{-3} (0.7 ppmv) at noon, compared with the average daytime satellite observed ozone of about 0.6 ppmv at the altitude of 0.003 mbar averaged between 40°N and 50°N in March [*Keating et al.*, 1996]. These calculated profiles are used as the background profiles of atmospheric trace gases. The profiles are assumed to be valid over the horizontal extent of the wave. The same set of chemical reactions in perturbation form is also used to calculate the trace species perturbations associated with the gravity wave, as described below.

3.2. Perturbation Model

A coupled linear inertiogravity wave model is used to estimate the gravity wave fluctuations of wind, temperature, and mixing ratios.

$$\frac{\partial u'}{\partial t} + u_0\frac{\partial u'}{\partial x} + v_0\frac{\partial u'}{\partial y} - fv' + \frac{\partial \phi'}{\partial x} = 0 \qquad (4a)$$

$$\frac{\partial v'}{\partial t} + u_0\frac{\partial v'}{\partial x} + v_0\frac{\partial v'}{\partial y} + fu' + \frac{\partial \phi'}{\partial y} = 0 \qquad (4b)$$

$$\frac{\partial u'}{\partial x} + \frac{\partial v'}{\partial y} + \frac{1}{\rho_0}\frac{\partial}{\partial z}(\rho_0 w') = 0 \qquad (4c)$$

$$\frac{\partial T'}{\partial t} + u_0\frac{\partial T'}{\partial x} + v_0\frac{\partial T'}{\partial y} + \beta^2 w' = \frac{1}{C_p}\left[\frac{\partial Q_0}{\partial T}T' + \sum_{k=1}^{J}\frac{\partial Q_0}{\partial q_{0,k}}q'_k\right] \qquad (4d)$$

$$\frac{\partial q'_j}{\partial t} + u_0\frac{\partial q'_j}{\partial x} + v_0\frac{\partial q'_j}{\partial y} + w'\frac{\partial q_{0,j}}{\partial z} = \frac{\partial}{\partial T}\left(\frac{P_{0,j} - L_{0,j}}{\rho_0}\right)T' + \sum_{k=1}^{J}\frac{\partial}{\partial q_{0,k}}\left(\frac{P_{0,j} - L_{0,j}}{\rho_0}\right)q'_k \qquad j = 1, 2, 3, \ldots, J \qquad (4e)$$

$$T' = \frac{H}{R}\frac{\partial \phi'}{\partial z}, \qquad (4f)$$

where ϕ is the geopotential, f is the Coriolis parameter, H is the atmospheric scale height, $\beta^2 = dT/dz + RT/(HC_p)$, C_p is the specific heat at constant pressure, and R is the gas constant. The diabatic heating and photochemical source rates are assumed to vary with temperature and species concentrations. The right-hand sides of (4d) and (4e) represent linear expansion of these variables, with Q_0 representing the background net diabatic heating rate and $P_{0,j}$ and $L_{0,j}$ representing the background photochemical production and destruction rates. Since the middle atmosphere is a system with strong coupling between radiation, dynamics, and chemistry, the diabatic heating and cooling and the photochemical reactions are coupled to the gravity wave model. If diabatic photochemical heating and cooling were ignored, (4a)-(4d) would describe the evolution of an adiabatic linear inertiogravity wave [*Andrews et al.*, 1987].

The net diabatic heating term Q_0 in (4d) is composed of photochemical (solar) heating and atmospheric cooling. The photochemical heating rate includes the contributions due to direct solar ultraviolet absorption and to exothermic chemical reactions. The methods used to calculate the chemical heating rates are described by *Brasseur and Offermann* [1986] and *Mlynczak and Solomon* [1993]. The calculation of longwave cooling rate uses the algorithm of *Fomichev et al.* [1996], which accounts for the radiation effects of CO_2, H_2O, and O_3 and the quenching of $CO_2(010)$ with $O(^3P)$.

We assume the existence of wave solutions of equations (4a)-(4f) of the form

$$(u', v', w', T', q'_j) = (u'_0, v'_0, w'_0, T'_0, q'_{j0}) \exp\left[i\omega t - i\,(k_x x + k_y y + k_z z) + \frac{z}{2H}\right] \qquad j = 1, 2, 3, \ldots, J, \qquad (5)$$

where ω is the frequency of the wave and k_x, k_y, and k_z are wavenumbers.

The substitution of (5) into the model equations (4) and the elimination of w' lead to $J+3$ (=22) coupled equations:

$$i\omega\vec{y} = A\vec{y},$$

where A is a (22 × 22) square matrix and $\vec{y}$ is a vector whose elements are the wave amplitudes u'_0, v'_0, ϕ'_0, and q'_{j0} (j = 1, 2, ..., J). For a given set of wavenumbers of k_x, k_y, and k_z values (specified), the frequency ω is obtained from the eigenvalues of matrix A. For a specified amplitude of temperature fluctuation T'_0 and for the gravity wave frequency ω calculated above, the substitution of (5) into (4a)-(4f) provides the perturbations of wind u', v', w' and the species mixing ratios q'_j. The choices of k_x, k_y, k_z, and T'_0 will be discussed in the next section. The gravity wave induced transport and photochemical reaction terms can be calculated from (3).

4. Calculation and Discussion

In order to calculate gravity wave fluctuations, background values of wind, temperature, and trace gas concentrations must first be determined. In the present calculations, the background wind velocities are chosen to be zero. The background temperature profile is taken from the U.S. Standard Atmosphere. The background atmospheric trace gas profiles are either specified (for the long-lived constituents) or calculated using a time-dependent one-dimensional photochemical model, as described above.

Wavelengths in three dimensions are needed as input to the gravity wave model. The rocket and radar data of the Structure and Atmospheric Turbulence Environment (STATE) experiment reported a wide range of vertical wavelength (2-30 km) near the mesopause. A typical horizontal wavelength is around 10^2-10^3 km [*Fritts et al.*, 1988]. Therefore, as a representative example, the vertical and horizontal wavelengths are taken as 10 and 1000 km, respectively, in the calculations.

Observations suggest that the variations of temperature induced by gravity waves in the mesosphere are typically 10-20 K, although larger amplitudes are not uncommon [*Theon et al.*, 1967; *Philbrick et al.*, 1985; *Schubert et al.*, 1990; *Zhang et al.*, 1993]. In the present calculations the amplitude of the temperature perturbation is taken to be $T_0' = 10$ K. This constrains the amplitude for all other perturbation variables, chemical as well as dynamical. The model solves for perturbation quantities at each altitude independently. The graphs that display perturbations as a function of altitude, to be discussed below, should be interpreted as the relative local impact that a gravity wave with 10-K amplitude would have and not as the vertical structure from a single wave. Therefore we can compare the magnitudes of the gravity wave induced chemical transport and photochemical reaction terms between different altitudes for gravity waves with the same amplitudes, and we can investigate at which altitudes the second-order gravity wave effects are important.

The amplitudes and phases of the gravity wave induced variations of $O(^3P)$, O_3, H, OH, and HO_2 during nighttime and daytime are shown in Figure 2. The relative amplitudes of several species fluctuations induced by gravity waves during nighttime have peaks near 80 km that can reach 2-3 times the background concentrations. This occurs in regions of very sharp vertical gradients in the $O(^3P)$ mixing ratio near the mesopause.

From (4e) we can see that the effect of gravity waves on minor atmospheric constituents is related to the product of the vertical dynamical perturbation w' and the vertical mixing ratio gradient $\partial q_{0,J}/\partial z$. In the case of $O(^3P)$, this gradient is largest near the mesopause (see Figure 1). The vertical gradient is particularly

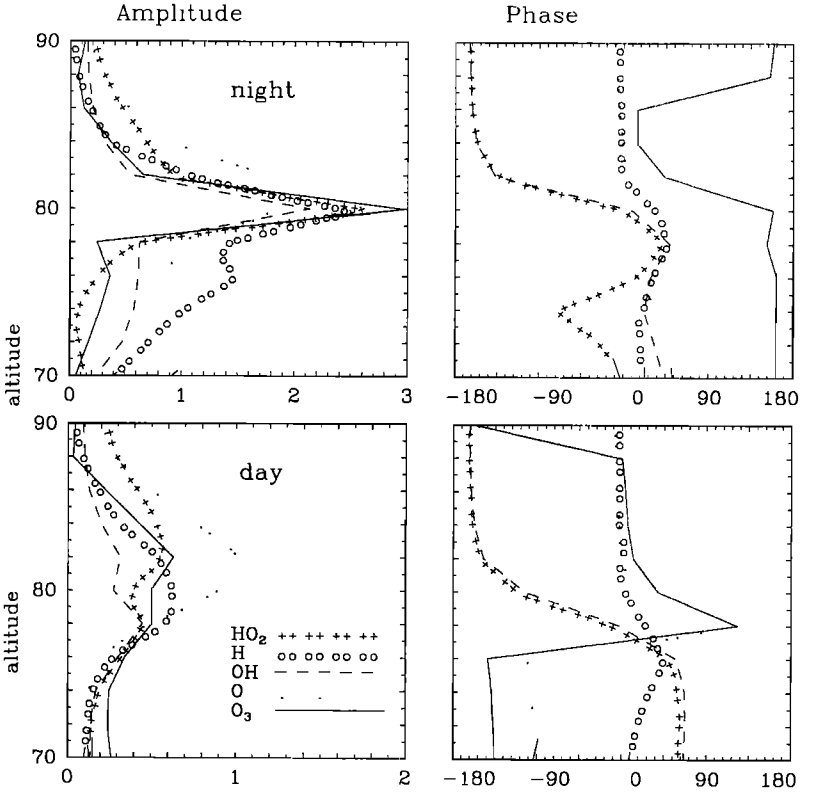

Figure 2. The relative amplitudes of the O_3, H, $O(^3P)$, OH, and HO_2 fluctuations induced by gravity waves and the phase differences (degrees) relative to the temperature fluctuations during (top) nighttime and (bottom) daytime. The amplitude of the temperature wave is 10 K at all altitudes.

large during nighttime because the concentration of $O(^3P)$ decreases very rapidly after sunset below about 80 km, where the photochemical time constant is much less than 1 hour. Above this level, the photochemical lifetime for atomic oxygen is long and the concentration remains almost unchanged over 24 hours. The effect of gravity waves on atomic oxygen is therefore expected to be largest in the vicinity of the mesopause during nighttime. Other minor atmospheric constituents will be indirectly influenced by gravity waves through photochemical reactions with atomic oxygen. In situ observations showing strong fluctuations in atomic oxygen concentration in the mesopause region [e.g., *Dickinson et al.*, 1985; *Offermann et al.*, 1981] provide supporting evidence for the large fluctuations calculated here.

Figure 2 indicates that in the daytime, the amplitudes of the fluctuations induced by gravity waves of $O(^3P)$, O_3, H, OH, and HO_2 are about 4 times smaller than they are at midnight. We can also see from Figure 2 that above and below the mesopause region, the amplitudes of chemical species variations induced by gravity wave are quite small.

These calculated variations are used to solve for the gravity wave induced tendencies to the mean composition. In order to assess their importance to the budget of the compounds, we compare the gravity wave tendencies with that due to vertical eddy diffusion. The vertical eddy diffusion coefficient is taken to be 10^6 cm^2 s^{-1} in the mesopause region [*Garcia and Solomon*, 1985; *Lübken*, 1997; *Lindzen*, 1981]. The gravity wave induced tendency terms and the eddy diffusion effect are shown for five species in the oxygen and hydrogen families for both night and day conditions (Figure 3). In these figures the gravity wave induced tendency terms and eddy diffusion term for each species have been divided by the mean concentration. They are as follows:

$$R_j = \frac{1}{q_{0,j}}\mathcal{R}_j, \quad T_j = \frac{1}{q_{0,j}}\mathcal{T}_j, \quad D_j = \frac{1}{q_{0,j}}\mathcal{D}_j,$$

and the units are in inverse seconds. The gravity wave induced photochemical reaction term R_j is, for some of these species, larger by as much as several orders of magnitude than the diffusion D_j and the gravity wave induced chemical transport T_j tendencies.

Figure 3 shows that the gravity wave tendencies for oxygen and hydrogen compounds are significant in the region of 75-90 km, where the amplitudes of chemical species induced by gravity waves are largest, but are small in other altitude regions of the atmosphere. This figure shows that the effect of diffusion on the atomic oxygen concentration is of the same order as that of the gravity wave induced photochemical reaction term. The distribution of atomic oxygen at about 80 km is therefore affected both by the dynamical process of diffusion and by nonlinearities in the photochemical reaction process. Atomic oxygen that is brought down through the mesopause, by whatever means, is rapidly destroyed by photochemistry. By advecting air down, gravity waves accelerate this process. In the narrow transition region between long and short photochemical lifetimes for atomic oxygen, gravity waves introduce a perturbation to the atomic oxygen density that impacts the production and loss rates of other trace species in the oxygen and hydrogen families. When advective transport by gravity waves is responsible, there is a correlation between perturbations of T and the $O(^3P)$ concentration that can both have direct impacts on the production and loss rates of other trace species. For O_3, OH, and HO_2, which have short lifetimes in this region, the diffusive timescale is longer than the photochemical timescale. Therefore their profiles are mainly determined by photochemistry and the gravity wave impacts are occurring through chemical interactions.

In order to investigate the overall importance of the gravity wave induced photochemical reaction and chemical transport effects and the vertical eddy diffusion for the distributions of trace gases, we compare R_j, T_j, and D_j with the relative photochemical loss rate $\mathcal{L}_j$, which is the inverse of the photochemical lifetime

$$\mathcal{L}_j = \frac{L_{0,j}}{q_{0,j}\rho_0}.$$

Table 1 gives the peak values of R_j, T_j, and D_j near 80 km and the value of $\mathcal{L}_j$ at the altitude of the R_j peak.

Table 1 shows that for a gravity wave with a temperature amplitude of 10 K, the values of R_j, $\mathcal{L}_j$, and D_j for atomic oxygen have the same order of magnitude near 80 km during night. This indicates that the distribution of atomic oxygen at about 80 km is controlled by diffusion, background photochemical reactions, and wave-induced photochemical reactions. In the same region, ozone is affected approximately equally by background and wave-induced photochemistry. During night the ozone distribution can therefore be modified when gravity waves pass through the mesopause region.

From Table 1 we can see that for $O(^3P)$, O_3, H, OH, and HO_2, the gravity wave induced transport terms are smaller than other tendency terms. The influence of gravity waves on these species distributions is mainly through nonlinear photochemical reactions. During day, when the background chemistry is more active and the atomic oxygen gradient is reduced, the magnitudes of the chemical species fluctuations induced by gravity waves are relatively small for all five species (see Figure 2).

A comment is necessary here on the large amplitude of the gravity wave induced changes. As noted in the discussion of Figure 2, the amplitudes of some of the chemical perturbations computed by the model exceed the background mixing ratios. This is clearly not physical because it can only be realized if the mixing ratio is negative over part of the wave period. It occurs because downward advection of atomic oxygen by the gravity wave in the vicinity of strongest gradients causes its concentration to increase severalfold over some wave phases. There is not a comparable decrease during the

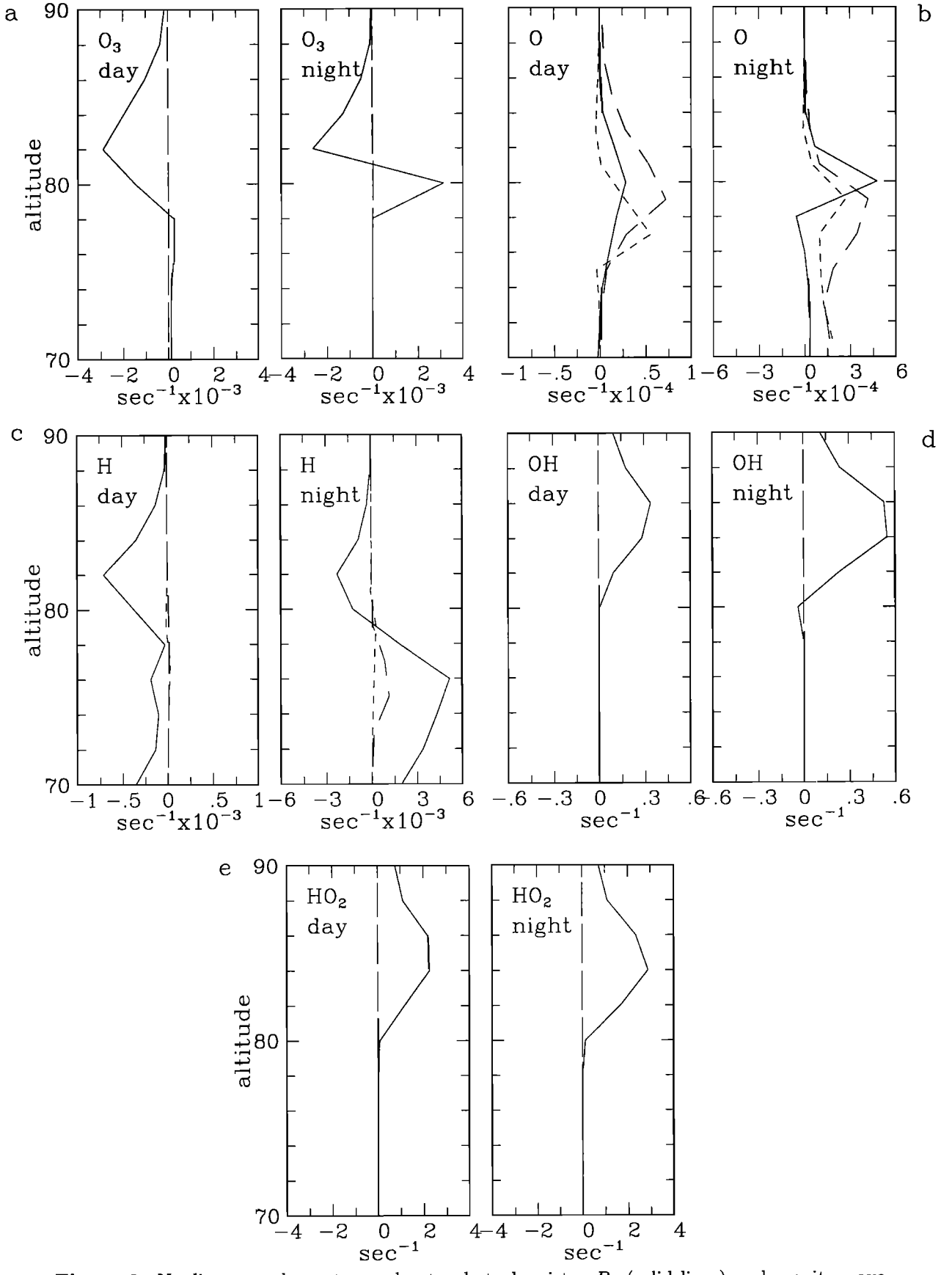

Figure 3. Nonlinear tendency terms due to photochemistry R_j (solid lines) and gravity wave advection T_j (short-dashed lines) and the diffusive tendency term D_j (long-dashed lines) for (a,b) oxygen and (c,d,e) hydrogen compounds at midday and midnight. Units are inverse second; note that scaling varies between frames.

Table 1. Maximum Values of Several Processes Near 80 km

			$T_0' = 10$ K			$T_0' = 20$ K	
Species	Time	$\mathcal{L}_j$, s^{-1})	R_j, s^{-1}	T_j, s^{-1}	D_j, s^{-1}	R_j, s^{-1}	T_j, s^{-1}
$O(^3P)$	midnight	0.49 (-3)	0.47 (-3)	0.27 (-3)	0.42 (-3)	0.19 (-2)	0.11 (-2)
	noon	0.23 (-3)	0.28 (-4)	0.56 (-4)	0.72 (-4)	0.11 (-3)	0.22 (-3)
O_3	midnight	0.13 (-2)	0.31 (-2)	0.35 (-4)	0.27 (-4)	0.13 (-1)	0.14 (-3)
	noon	0.15 (-1)	0.29 (-2)	0.44 (-4)	0.20 (-4)	0.11 (-1)	0.18 (-3)
H	midnight	0.34 (-2)	0.23 (-2)	0.30 (-3)	0.12 (-2)	0.90 (-2)	0.12 (-2)
	noon	0.28 (-2)	0.71 (-3)	0.32 (-4)	0.18 (-4)	0.28 (-2)	0.13 (-3)
OH	midnight	0.38 (1)	0.55 (0)	0.67 (-4)	0.51 (-4)	0.22 (1)	0.27 (-3)
	noon	0.88 (1)	0.34 (0)	0.31 (-4)	0.28 (-4)	0.14 (1)	0.12 (-3)
HO_2	midnight	0.80 (1)	0.29 (1)	0.62 (-4)	0.11 (-3)	0.12 (2)	0.25 (-3)
	noon	0.10 (2)	0.23 (1)	0.38 (-4)	0.57 (-4)	0.91 (1)	0.15 (-3)

Read 2.0(3) as 2.0×10^3.

upward advection phase of the wave because the gradient dies out rapidly in the vertical. Since the linear equations used here do not permit the background concentration to vary, the local maxima and minima lead to amplitudes greater than 1 and therefore to apparent negative mixing ratios. This situation is a result of two factors: the linearity of the model and the assumed sinusoidal form of the chemical perturbations. The solution can distort the calculation of the nonlinear gravity wave tendencies if the perturbation chemistry field is not realistic. To account for this effect in the model, we have recalculated these nonlinear tendency terms with the following adjustment: wherever in the wave the sum of the background and perturbation concentrations indicates a negative mixing ratio, we have replaced the mixing ratio by zero. This will tend to reduce the magnitude of the nonlinear terms, with a maximum reduction of a factor of two where the perturbation is much larger than the mean concentration. Figure 4 shows an example of the reduction in the nonlinear photochemical tendency induced by gravity wave for ozone during night. Reductions of the other nonlinear terms are comparable.

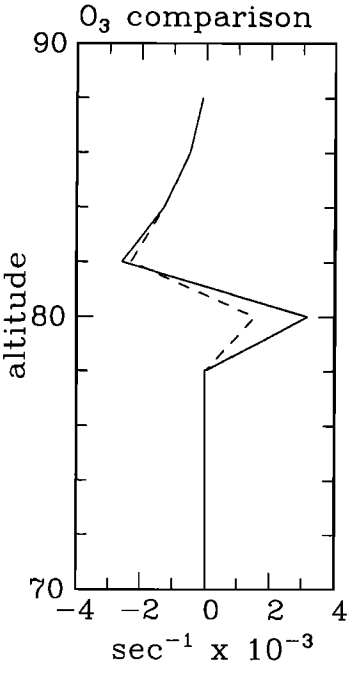

Figure 4. Comparison of the second-order gravity wave photochemical effect R_{O_3} for ozone. The solid line is calculated using equation (6); the dashed line is calculated with all concentrations constrained to be nonnegative.

The above mentioned calculations are for temperature fluctuations with an amplitude of T_0' of 10 K, which is about 5% of the background temperature. The observations show that the typical range of root-mean-square values of T'/T_0 is 0.05-0.1 for the region around 80 km, while values of $T'/T_0 \geq 0.15$ are not uncommon [*Theon et al.*, 1967; *Philbrick et al.*, 1985]. When repeated for $T_0' = 20$ K (summarized in Table 1), the calculations show that the magnitudes of the gravity wave induced chemical transport and photochemical reaction terms are about 4 times their values in the previous case, and now the gravity wave induced photochemical reaction effects exceed the background photochemical tendencies during nighttime. During daytime, the gravity wave induced photochemical reaction tendencies of the five species (R_j) are approximately equal in magnitude to the background photochemical rates $\mathcal{L}_j$. The fourfold increase comes about because when T_0' is doubled, the amplitudes of all perturbation quantities, u_0', v_0', and w_0' as well as q_{j0}', are also doubled because the gravity wave model is linear. The second-order gravity wave induced changes, which result from the product of two perturbation quantities, will rise by factors of 4. This means that when the amplitude of gravity waves is large, their impact on the distribution of trace gases in the region of the mesopause is magnified.

5. Summary

Gravity waves can influence the profiles of trace gases through nonlinear effects even if the gravity waves are not breaking. For atomic oxygen, which has a rela-

tively long photochemical lifetime near the mesopause, the net changes due to gravity wave induced chemical transport, gravity wave induced photochemical reaction changes, and vertical diffusion have comparable magnitudes. However, the model presented here indicates that gravity waves can also have an influence on species with short photochemical lifetimes through the gravity wave induced nonlinearities in chemical sources, which can be much larger than the gravity wave advection and diffusion effects. For ozone and reactive hydrogen compounds, the net tendency associated with gravity wave induced photochemical reaction effects is comparable to the photochemical tendency associated with the background field. Therefore gravity waves can affect the distributions of these species even though these species are in approximate photochemical equilibrium near the mesopause. Because the gravity wave induced changes to the photochemistry do not necessarily act to reduce the background gradients of the trace constituents, the gravity wave influence cannot be represented by an effective diffusion coefficient.

The influence of gravity waves on atmospheric minor constituent distributions near the mesopause is greater during nighttime than during daytime. This is primarily because the vertical gradient of the $O(^3P)$ mixing ratio is greater during nighttime than during daytime. The perturbations in mixing ratios of other trace gases that react strongly with atomic oxygen are also largest during nighttime. In addition, during daytime, the lifetimes of some species are shorter and so the relative impact of gravity waves on trace gas distributions is smaller.

Table 1 and Figure 3 indicate that for individual species with short chemical lifetimes, the changes due to gravity wave induced photochemical perturbations are much greater than those due to diffusion. However, this result does not contradict previous studies that showed that diffusion is very important in the mesopause region. The diffusion due to breaking gravity waves can influence the distribution of the chemical families, O_x and HO_x, whose photochemical lifetimes are much longer than those of the individual family members [*Brasseur and Solomon*, 1986]. We calculated the gravity wave induced photochemical reaction terms and diffusion terms of the oxygen family O_x and the hydrogen family HO_x. For both the O_x and HO_x families these contributions are comparable in magnitude to those due to the gravity wave induced photochemical reaction term. Therefore both diffusion and gravity wave induced photochemical perturbations can influence the distributions of these chemical families in the mesopause region; the latter also affects the partition among the family members.

The results presented here indicate that for a gravity wave with 10-K amplitude, the atomic oxygen tendency due to mean vertical diffusion is comparable in magnitude to that due to nonlinear effects associated with gravity waves. However, several studies suggest that the vertical eddy diffusion coefficient K_z is about an order of magnitude smaller than the value adopted here (10^6 cm^2 s^{-1}) [*Brasseur and Offermann*, 1986; *Strobel et al.*, 1987; *Bevilacqua et al.*, 1990]. In addition, the temperature amplitude associated with gravity waves can occasionally be larger than 10 K. Our calculation indicates that the impact of gravity waves on the distributions of trace gases in the mesopause region depends roughly on the square of the wave amplitude. Therefore the nonlinear effects of propagating gravity waves can in some circumstances and locations be the dominant contributor to the net tendency of the mean atomic oxygen concentration.

Finally, it should be stressed that the dynamical-photochemical gravity wave model in this paper is a linear model, which has some intrinsic limitations. First, the linear model does not permit the background concentration to vary. Second, the linear perturbation equation does not account for conservation of mass of the constituents, so that negative mixing ratios are mathematically allowed and in the present study, are computed by the model. The primary effect of this unphysical situation for the conclusions is that it leads to an overprediction of the net impact of the gravity waves on the mean distribution. This overprediction is small over much of the mesosphere ($< 25\%$) and never more than a factor of two. Even when accounting for this effect, one can conclude that gravity waves have a significant impact on the distributions of chemical species in the mesopause region through nonlinear processes.

Acknowledgments. The authors thank V. Fomichev for providing his model of atmospheric cooling rate. The authors would like to acknowledge comments by Rolando Garcia and Douglas Kinnison. This research was supported by project "Storm 23" of the Chinese Academy of Sciences and the National Science Foundation of China (49990454). The National Center for Atmospheric Research is supported by the National Science Foundation.

References

Allen, M., Y. L. Yung, and J. W. Waters, Vertical transport and photochemistry in the terrestrial mesosphere and lower thermosphere (50-120 km), *J. Geophys. Res., 86*, 3617-3627, 1981.

Andrews, D. G., and M. F. McIntyre, Planetary waves in horizontal and vertical shear: The generalization of the Eliassen-Palm relation and the mean zonal acceleration, *J. Atmos. Sci., 33*, 2031-2046, 1976.

Andrews, D. G., J. R. Holton, and C. B. Leovy, *Middle Atmosphere Dynamics*, Academic, San Diego, Calif., 1987.

Bevilacqua, R. M., D. F. Strobel, M. E. Summers, J. J. Olivero, and M. Allen, The seasonal variation of water vapor and ozone in the upper mesosphere: Implications for vertical transport and ozone photochemistry, *J. Geophys. Res., 95*, 883-894, 1990.

Brasseur, G., and D. Offermann, Recombination of atomic oxygen near the mesopause: Interpretation of rocket data, *J. Geophys. Res., 91*, 10,818-10,824, 1986.

Brasseur, G., and S. Solomon, *Aeronomy of the Middle Atmosphere*, 2nd ed., 452 pp., D. Reidel, Norwell, Mass., 1986.

DeMore, W. B. et al., Chemical kinetics and photochemical data for use in stratospheric modeling, Eval. 12, *JPL Publ. 97-4*, 266 pp., 1997.

Dickinson, P. H. G., U. von Zahn, K. D. Baker, and D. B. Jenkins, Lower thermosphere densities of N_2, O and Ar under high latitude winter conditions, *J. Atmos. Terr. Phys.*, *47*, 283-290, 1985.

Dunkerton, T. J., Wave transience in a compressible atmosphere, part III, The saturation of internal gravity waves in the mesosphere, *J. Atmos. Sci.*, *39*, 1042-1051, 1982.

Eckermann, S. D., D. E. Gibson-Wilde, and J. T. Bacmeister, Gravity wave perturbations of minor constituents: A parcel advection methodology, *J. Atmos. Sci.*, *55*, 3521-3539, 1998.

Fomichev, V. I., W. E. Ward, and C. McLandress, Implications of variations in the 15 μm CO_2 band cooling in the mesosphere and lower thermosphere associated with current climatologies of the atomic oxygen mixing ratio, *J. Geophys. Res.*, *101*, 4041-4055, 1996.

Fritts, D. C., Gravity wave saturation in the middle atmosphere: A review of theory and observations, *Rev. Geophys.*, *22*, 275-308, 1984.

Fritts, D. C., S. A. Smith, B. B. Balsley, and C. R. Philbrick, Evidence of gravity wave saturation and local turbulence production in the summer mesosphere and lower thermosphere during the STATE experiment, *J. Geophys. Res.*, *93*, 7015-7025, 1988.

Fritts, D. C., J. R. Isler, J. H. Hecht, R. L. Walterscheid, and O. Andreassen, Wave breaking signatures in sodium densities and OH airglow, 2, Simulation of wave and instability structures, *J. Geophys. Res.*, *102*, 6669-6684, 1997.

Garcia, R. R., and S. Solomon, The effect of breaking gravity waves on the dynamical and chemical composition of the mesosphere and lower thermosphere, *J. Geophys. Res.*, *90*, 3850-3868, 1985.

Keating, G. M., L. S. Chiou, and N. C. Hsu, Improved ozone reference models for the COSPAR international reference atmosphere, *Adv. Space Res.*, *18*, 11-58, 1996.

Lindzen, R. S., Turbulence and stress due to gravity wave and tidal breakdown, *J. Geophys. Res.*, *86*, 9707-9714, 1981.

Llewellyn, E. J., and I. C. McDade, A reference model for atomic oxygen in the terrestrial atmosphere, *Adv. Space Res.*, *18*, 209-226, 1996.

Lübken, F.-J., Seasonal variation of turbulent energy dissipation rates at high latitudes as determined by in situ measurements of neutral density fluctuations, *J. Geophys. Res.*, *102*, 13,441-13,456, 1997.

Makhlouf, U. B., R. H. Picard, and J. R. Winik, Photochemica dynamical modeling of the measured response of airglow to gravity waves, 1, Basic model for OH airglow, *J. Geophys. Res.*, *100*, 11,289-11,311, 1995.

Makhlouf, U. B., R. H. Picard, J. R. Winik, and T. F. Tuan, A model for the response of the atomic oxygen 557.7 nm and the OH Meinel airglow to atmospheric gravity waves in a realistic atmosphere, *J. Geophys. Res.*, *103*, 6261-6269, 1998.

Mlynczak, M. G., and S. Solomon, A detail evaluation of the heating efficiency in the middle atmosphere, *J. Geophys. Res.*, *98*, 10,517-10,541, 1993.

Offermann, D., V. Friedrich, P. Ross, and U. von Zahn, Neutral gas composition measurements between 80 and 120 km, *Planet. Space Sci.*, *29*, 747-764, 1981.

Philbrick, C. R., F. J. Schmidelin, K. U. Grossman, G. Lang, D. Offermann, K. D. Baker, D. Krankowsky, and U. von Zahn, Density and temperature structure over northern Europe. *J. Atmos. Terr. Phys.*, *47*, 159-172, 1985.

Schoeberl, M. R., D. F. Strobel, and J. P. Apruzese, A numerical model of gravity wave breaking and stress in the mesosphere, *J. Geophys. Res.*, *88*, 5249-5259, 1983.

Schubert, G., R. L. Walterscheid, J. H. Hecht, and G. G. Sivjee, Temperature gradients at mesopause heights inferred from OH nightglow data, *J. Geophys. Res.*, *95*, 19,061-19,067, 1990.

Smith, S. A., D. C. Fritts, and T. E. VanZandt, Evidence for a saturated spectrum of atmospheric gravity waves, *J. Atmos. Sci.*, *44*, 1404-1410, 1987.

Strobel, D. F., Parameterization of linear wave chemical transport in planetary atmospheres by eddy diffusion, *J. Geophys. Res.*, *86*, 9806-9810, 1981.

Strobel, D. F., M. E. Summer, R. M. Bevilacqua, M. T. Deland, and M. Allen, Vertical constituent transport in the mesosphere, *J. Geophys. Res.*, *92*, 6691-6698, 1987.

Swenson, G. R., and C. S. Gardner, Analytical models for the response of the mesospheric OH* and Na layers to atmospheric gravity waves, *J. Geophys. Res.*, *103*, 6271-6294, 1998.

Theon, J. S., W. Nordberg, L. B. Katchen, and J. J. Horvath, Some observations on the thermal behavior of the mesosphere, *J. Atmos. Sci.*, *24*, 428-438, 1967.

Walterscheid, R. L., and G. Schubert, Gravity wave fluxes of O_3 and OH at the nightside mesopause, *Geophys. Res. Lett.*, *16*, 719-722, 1989.

Walterscheid, R. L., G. Schubert, and J. M. Strans, A dynamical-chemical model of wave-driven fluctuations in the OH nightglow, *J. Geophys. Res.*, *92*, 1241-1254, 1987.

Weinstock, J., Saturated and unsaturated spectra of gravity waves and scale-dependent diffusion, *J. Atmos. Sci.*, *47*, 2211-2225, 1990.

Zhang, S. P., R. H. Peterson, R. H. Wiens, and G. G. Shepherd, Gravity waves from O_2 nightglow during the AIDA '98 Campaign I: Emission rate/temperature observation, *J. Atmos. Terr. Phys.*, *55*, 355-375, 1993.

G. P. Brasseur, Max Planck Institute for Meteorology, Bundestrasse 55, 20146 Hamburg, Germany. (brasseur@dkrz.de)

A. K. Smith, National Center for Atmospheric Research, P.O. Box 3000, Boulder, CO 80307. (aksmith@ucar.edu)

J. Xu, Laboratory of Numeric Study of Heliospheric Physics, Center for Space Science and Applied Research, Chinese Academy of Sciences, Beijing 100080, China. (xurrjy@center.cssar.ac.cn)

(Received March 9, 2000; revised June 26, 2000; accepted July 21, 2000.)